DOI: 10.1002/chem.200501551

Interactions of Neutral and Cationic Transition Metals with the Redox System of Hydroquinone and Quinone: Theoretical Characterization of the Binding Topologies, and Implications for the Formation of Nanomaterials**

Hai-Bo Yi,[a, b] Martin Diefenbach,[a, b] Young Cheol Choi,[a] Eun Cheol Lee,[a] Han Myoung Lee,[a] Byung Hee Hong,[a, c] and Kwang S. Kim*[a]

Abstract: To understand the self-assembly process of the transition metal (TM) nanoclusters and nanowires self-synthesized by hydroquinone (HQ) and calix[4]hydroquinone (CHQ) by electrochemical redox processes, we have investigated the binding sites of HQ for the transition-metal cations $TM^{n+} = Ag^+$, Au^+, Pd^{2+}, Pt^{2+}, and Hg^{2+} and those of quinone (Q) for the reduced neutral metals TM^0, using ab initio calculations. For comparison, TM^0–HQ and TM^{n+}–Q interactions, as well as the cases for Na^+ and Cu^+ (which do not take part in self-synthesis by CHQ) are also included. In general, TM–ligand coordination is controlled by symmetry constraints imposed on the respective orbital interactions. Calculations predict that, due to synergetic interactions, silver and gold are very efficient metals for one-dimensional (1D) nanowire formation in the self-assembly process, platinum and mercury favor both nanowire/nanorod and thin film formation, while palladium favors two-dimensional (2D) thin film formation.

Keywords: ab initio calculations · hydroquinone · metal-cation–π interactions · nanowires · transition metals

Introduction

Noncovalent interactions play a dominant role in many forefront areas of modern chemistry and biology.[1] One such example is the cation–π interaction, which now has been characterized in a wide range of contexts.[2–12] Interest in designing superfunctional materials involving these noncovalent interactions has grown dramatically during the past few decades.[13–16] Recently, Hong et al. reported self-assembled arrays of calix[4]hydroquinone (CHQ) nanotubes and self-synthesized metal nanoclusters, nanowires, and nanostructures.[17,18] In this self-synthesis process, transition-metal cations TM^{n+} can be bound inside (or outside) the CHQ nanotubes, and the redox reaction toward oxidized calix[4]quinones (CQ) yields reduced transition-metal nanowires (or thin films): $CHQ + 8/nTM^{n+} \rightarrow CQ + 8/nTM + 8H^+$. Understanding this mechanism is of importance for the self-synthesis of nanowires using organic molecular systems.

Since each CHQ has four hydroquinone (HQ) moieties, and CQ has four quinone (Q) moieties, we may consider these monomeric units as a part of the model system, in which the overall electrochemical reaction is $HQ + 2/nTM^{n+} \rightarrow Q + 2/nTM + 2H^+$. In this process, the reduction potential E^0 for $Q + 2H^+ + 2e^- \rightarrow HQ$ is -0.70 V in aqueous solution. The reduction potential of this model system also applies to the "real" TM^{n+}/CHQ nanosystems, because the spontaneous redox process in aqueous solution is observed only in five metal cation systems with $E^0 < -0.70$ V, that is, Ag^+, Au^+, Pd^{2+}, Pt^{2+}, and Hg^{2+}, where the E^0 values are -0.80, -1.69, -0.95, -1.12, and -0.85 V, respectively. The spontaneous reduction does not take place for Cu^+, because its E^0 value is -0.52 V, and is thus less negative than that of Q. There is, however, no direct relation between the magnitude

[a] Dr. H.-B. Yi, Dr. M. Diefenbach, Y. C. Choi, E. C. Lee, Dr. H. M. Lee, Dr. B. H. Hong, Prof. Dr. K. S. Kim
Center for Superfunctional Materials
Department of Chemistry
Pohang University of Science and Technology
San 31, Hyojadong, Namgu, Pohang 790–784 (Korea)
Fax: (+82) 54-279-8137
E-mail: kim@postech.ac.kr

[b] Dr. H.-B. Yi, Dr. M. Diefenbach
Contributed equally to this work.

[c] Dr. B. H. Hong
Current address: Department of Physics, Columbia University, 538 West 120th Street, New York, NY 10027 (USA)

[**] Contribution from the National Creative Research Initiative Center for Superfunctional Materials.

of the resulting redox potential and the efficiencies of the observed redox reactions for the nanowire formation. While, for example, uniformly aligned silver nanowire arrays are formed with Ag^+ in a fast redox reaction that releases -0.1 V, the experiment suggests that the reduction of Pd^+ yields only thin layers of metallic palladium, though the overall redox potential is more negative ($\Delta E^0 = -0.25$ V).

To understand the self-synthesis and self-assembly phenomena of this nanomaterial, it is essential to investigate the interactions of HQ and Q with the transition-metal cations and the reduced neutral metal atoms. Furthermore, the cation–HQ/Q model system plays an important role in chemistry and biology due to the strong electron-donating/accepting abilities, for example, as electron carriers through π backdonation.[19–22] Therefore, an investigation of transition-metal binding with π systems such as quinoid molecules is important in a more general context, that is, for understanding the basis of metal-promoted transformations of aromatic compounds, which may lead to the design of novel nanomaterials.

In the present work, we discuss the interactions between the ring compounds (HQ and Q) and transition-metal cations ($TM^{n+} = Ag^+$, Au^+, Pd^{2+}, Pt^{2+}, and Hg^{2+}) and their neutral counterparts by using ab initio calculations. For comparison, the metal cations Na^+ and Cu^+ as well as the ligand benzene (Bz) are also included, and Na is included in the TM notation for convenience. We investigate the conformational structures, binding sites, and binding energies, which are essential for understanding of the self-assembly process of the transition-metal nanoclusters, nanowires and nanofilms self-synthesized from HQ/CHQ by electrochemical redox processes. Furthermore, implications from energy changes with respect to the redox process are discussed.

Computational Details

All calculations were performed at the MP2(full) level of theory.[23] Dunning's correlation consistent basis sets[24] were employed, that is, aug-cc-pVDZ for the non-metal elements C, H, and O, and cc-pCVDZ for Na. For the remaining metal centers, the scalar relativistic pseudopotentials (MWB) of the Stuttgart–Dresden–Bonn type were used, replacing 10 (Cu),[25] 28 (Pd, Ag),[26] or 60 (Pt, Au, Hg)[26] core electrons. The valence space was described by the corresponding (8s7p6d)/[6s5p3d] basis sets. This basis-set combination is abbreviated as aVDZ. All minima were identified through analysis of the Hessian matrix from frequency calculations.

Interaction energies were determined by calculating MP2-(full)/aVTZ single points on the optimized MP2/aVDZ minimum geometries. For the aVTZ basis set, a set of two f and one g polarization functions were added to the valence basis set of the transition-metal atoms (Cu, Pd, Ag, Pt, Au, Hg),[27] the cc-pCVTZ basis set was used for Na, and the aug-cc-pVTZ basis set was employed for C, H, and O. Basis set superposition error (BSSE) corrections were done with the counterpoise method.[28] Zero-point energy (ZPE) corrections were made using the MP2/aVDZ frequency calculations. All numbers reported here refer to this MP2(full)/aVTZ//MP2(full)/aVDZ approach with interaction energies including ZPE and BSSE corrections. The basis sets and pseudopotentials were retrieved from the EMSL Basis Set Library.[29] Charges were calculated based on natural bond orbital (NBO) analysis.[30]

Results and Discussion

We have considered four different conformations for the binding of TMs with HQ/Bz/Q (Figure 1). π_{cen} denotes centrosymmetric η^6-coordinate complexes (η^4 in the case of TM-Q), π_{off} denotes complexes in which the TM coordinates off-center towards the perimeter of the ring; π_C stands for η^3 coordination (located above a single carbon of Bz), and σ_O stands for coordination to an oxygen lone pair of HQ or Q. In the following, the conformations for the binding of the cationic/neutral TM with HQ and Q are discussed. Where applicable, comparisons to the most stable TM–Bz complexes are made.

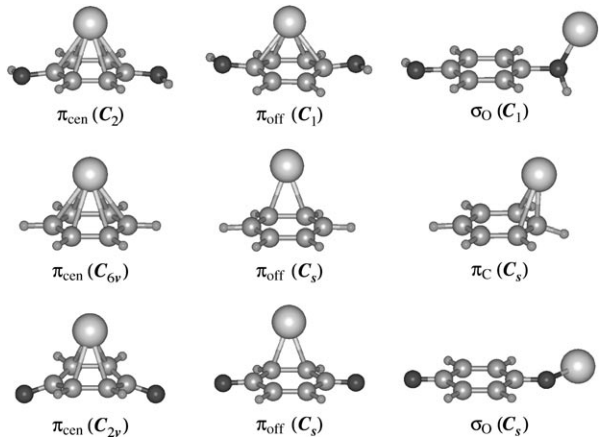

Figure 1. Binding sites of TM^{n+} complexes with HQ (top), Bz (middle), and Q (bottom). Symmetries are given in parentheses. Note that the TM–OH plane is perpendicular to the ring plane in σ_O-bound TM^{n+}–HQ.

Binding of TM^{n+} to HQ: In the initial stage of the self-assembly within the redox process, a metal cation interacts with a HQ moiety. A metal cation may bind to HQ either by coordinating to the π face (ring site) or to a lone pair of an oxygen atom (O site). The general aspect of oxygen versus ring binding was discussed previously for singly charged 3d transition-metal cations with phenol.[31] In these systems, the ring binding site is found to be favored over the O binding site. Differences in bond strength (to the ring site) among the 3d series are reflected by the difference in binding energies (BEs) of the corresponding TM^+–(C_6H_6) complexes.

In transition-metal-cation–arene complexes,[32] the π-bonding to an aromatic ligand L is generally discussed in terms of the L→TM π–d donation and the TM→L d–π* backdonation.[33,34] For main-group cations, the bonding situation is simpler than for transition-metal cations, as the bonding is dominated by purely electrostatic contributions, that is, charge–dipole and charge–quadrupole interactions. The interaction of Na^+ with HQ, for example, results in a moderate binding energy of 23–24 kcal mol^{-1} (Table 1) with no distinct preference for either the ring site or the O site. The 3d transition metal cation Cu^+ on the other hand clearly favors a π_{cen} coordination at the ring site with a much larger binding energy of 60.4 kcal mol^{-1}, reflecting π back-bonding contributions. The σ_O-bound isomer is 17 kcal mol^{-1} less favorable in energy (43.5 kcal mol^{-1}).

Like Cu^+, the Ag^+ and Au^+ cations also favor a ring-bound conformation over a σ_O coordination, which again is due to the additional L←TM π backdonation in the π-bound complex. For $Ag(HQ)^+$, there is not even a minimum for σ_O coordination; rather, the silver ion moves downhill on the energy surface towards the ring site. The structural features in the two lighter complexes, $Cu(HQ)^+$ and $Ag(HQ)^+$ are still governed by strong electrostatic character of the bonding in these complexes. Au^+ on the other hand stands out and prefers a π_{off} coordination outside the center on the perimeter of the ring. This deviation from a central position in the cationic gold complex is also observed for the corresponding benzene complex (Table 1). Such a phenomenon is ascribable to symmetry restrictions, as has been shown previously by Dargel et al.[35]

In the Au^+–HQ case, the situation may be characterized as follows. Owing to the d^{10} occupation in the noble metal cation, the L→TM p_π–d_π donation is not straightforward. A π_{cen} structure in $TM(HQ)^+$ is C_2-symmetric; Figure 2 shows a schematic representation of the relevant orbital symmetries. While the L←TM π* backdonation is viable from the doubly occupied d_{xy} and $d_{x^2-y^2}$ orbitals into the empty LUMO orbitals of matching symmetry, there are restrictions for donations from the ligand to the electron-deficient metal. Within C_2 symmetry, the highest occupied π MO of HQ (belonging to the b irreducible representation) may not interact with the empty 6s orbital (because it is of different symmetry) of the metal cation. Upon changing from C_2 symmetry to C_1, no such limitations exist, and the highest occupied HQ orbitals now all transform into the "a" representation, such that the HOMO of HQ can interact with the 6s(a) orbital of Au. As a consequence, the electron transfer from HQ to Au^+ is possible, because the relativistic effects dramatically lower the energy of the 6s orbital, making it highly electrophilic.[36] Accordingly, in the C_1-symmetric $Au(HQ)^+$ complex, the substantial s-orbital occupation along with considerable charge transfer is observed, and the partial charge on the ligand amounts to $q(HQ) = 0.31$.

The charge transfer from a neutral ligand L to a cationic metal TM^+ is only possible in appreciable amounts if the ionization energy $IE(L) \leq IE(TM)$. Thus, in the other TM^+–HQ complexes, the charge transfer

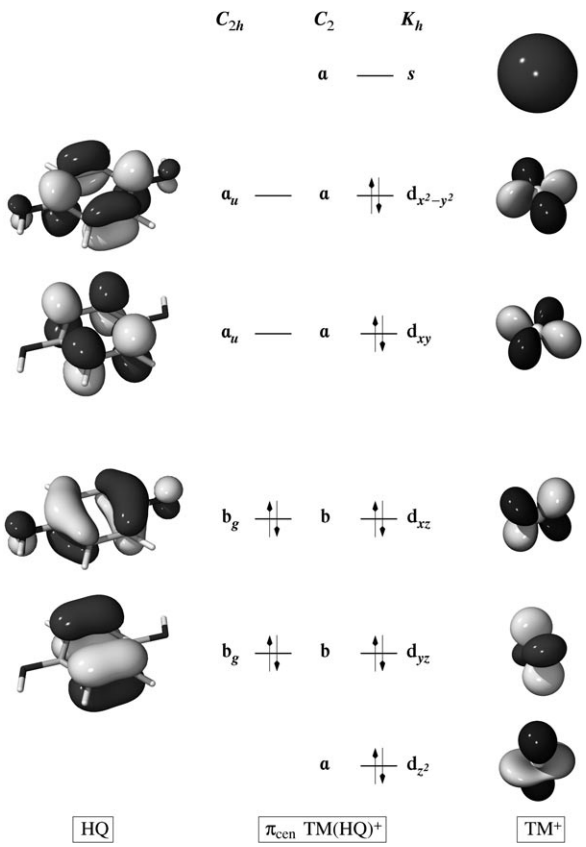

Figure 2. Schematic molecular orbital diagram for a TM–HQ complex. A C_{2h}-symmetric HQ ligand has two π-type HOMOs of b_g symmetry and two π-type LUMOs of a_u symmetry. In a π_{cen} C_2-symmetric complex, these transform into the b and a irreducible representations, respectively. Similarly, the atomic s and d orbitals of the TM transform into either a or b irreducible representation, which may then overlap with the ligand's orbitals of matching symmetry.

Table 1. Binding energies in kcal mol^{-1} of TM^{n+}–L complexes (L = HQ, Bz, Q) including ZPE contributions and BSSE corrections, calculated at the MP2/aVTZ//MP2/aVDZ level of theory. Values are given only for structures that correspond to local minima. Boldface entries indicate lowest energy structures.

(TM^{n+}–L)	L = HQ			L = Bz			L = Q		
	π_{cen}	π_{off}	σ_O	π_{cen}	π_{off}	π_C	π_{cen}	π_{off}	σ_O
^{1}(Na^+–L)	23.1		**23.6**	**21.7**[a]			4.5	4.5	**25.6**
^{1}(Cu^+–L)	**60.4**		43.5	**57.2**[b]			31.4	35.4	**47.5**
^{1}(Ag^+–L)	**42.3**			**40.9**[c]			21.9	25.0	**34.3**
^{1}(Au^+–L)	56.8	**71.7**	43.2	55.0	**67.1**[d]	66.2	41.5	**56.1**	51.1
^{1}(Pd^{2+}–L)	**239.3**	237.1	232.8		**196.3**		**176.4**		91.2
^{1}(Pt^{2+}–L)	249.8	**258.7**	218.6		**224.5**	204.7	**213.3**	162.9	141.3
^{1}(Hg^{2+}–L)	125.6	144.7	**172.1**	126.3	129.0	**129.5**	92.7	88.1	**122.5**
^{3}(Pd^{2+}–L)	**215.3**	204.2			**182.5**		**117.4**	107.0	
^{3}(Pt^{2+}–L)	**238.2**	220.1			**209.7**		**188.4**	175.8	

[a] Exptl 22.1 ± 1.4, ref. [47]. [b] Exptl 52 ± 5, ref. [48]. [c] Exptl 37.4 ± 1.7, ref. [49]. [d] Exptl 69 ± 7, ref. [50].

is only small (q(HQ) ≤ 0.02), which is in line with the ionization energy of HQ (7.99 eV)[37] versus those of Na, Cu, Ag, and Au, which are 5.14, 7.73, 7.59, and 9.23 eV, respectively.[38]

For analogous reasons as above, the binding properties of TM^+–HQ are mirrored in the corresponding TM^+–Bz complexes, in which the monocations Na^+, Cu^+, and Ag^+ are π_{cen} coordinated, whereas Au^+ binds in a η^2 fashion to the perimeter of the ring. The charge transfer in the TM^+–Bz complex is again only noticeable in the gold complex (q(Bz) = 0.21); it is smaller than in the TM^+–HQ complex, due to the higher IE of benzene (9.24 eV).[37]

An η^2 complex with benzene is sixfold degenerate. With a ligand like HQ, however, there are two energetically different π_{off} sites for complexation above a C–C bond due to the lower symmetry of the HQ ligand, that is, one with TM^{n+} sitting above C1–C2 (in the proximity to the OH group, Figure 3a) and one above C2–C3 (Figure 3b). If π_{off} coordinated, most of the cations studied here prefer binding to C2–C3 because of better p_π–d_{xz} overlap—the metal sits above the nodal plane such that the two d_{xz} lobes with opposite sign overlap with the matching π lobes of the ligand's HOMO. Only those metals with a full d^{10} shell and a highly electrophilic 6s orbital bind to C1–C2, such that a single 6s lobe may overlap with a π lobe of the same sign. Accordingly, the latter is preferable for the gold cation and for the π_{off}-bound mercury dication, due to favorable p_π–6s overlap.

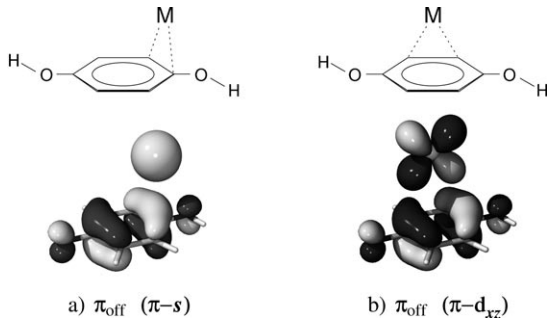

Figure 3. Binding scenarios of π_{off} TM^{n+} complexes with HQ. Orbitals which may overlap are schematically shown. a) π(HQ) HOMO matches an s(TM) orbital, and b) π(HQ) HOMO matches a d_{xz}(TM) orbital.

In the π-bound Na^+–HQ system, the metal–ligand distance is 249 pm (Table 2), and the charge induced ion–dipole interactions afford a ZPE corrected binding energy of D_0 = 23.1 kcal mol^{-1}. The cationic copper–HQ complex is much more compact with a metal–ligand distance of only 170 pm—although the ionic radii[39] of Na^+ (95 pm) and Cu^+ (96 pm) are nearly identical—and it yields a much stronger binding energy of D_0 = 60.4 kcal mol^{-1}, which is partly due to the L←TM π-backdonation. Owing to the larger ionic radius of Ag^+ (126 pm) compared to Cu^+, the metal–ligand distance increases to 211 pm such that the binding energy of Ag^+–HQ is smaller and amounts to D_0 = 42.7 kcal mol^{-1}. In the heavier cationic gold complex, the metal–ligand distance is 200 pm and thus shorter than in the silver complex, even though the ionic radius of Au^+ is 137 pm and thus larger than that of Ag^+. Relativistic contraction of the 6s orbital along with destabilization of the 5d shell to permit better d_π–p_π overlap for backbonding affords a strong interaction with covalent character.[40] Therefore, both the L→TM σ donation into the Au(6s) orbital and the L←TM π backdonation from the Au(5d) orbitals are large, and the binding energy amounts to 71.7 kcal mol^{-1}. The features of the π-bound monocationic TM^+–HQ structures by and large resemble those of their benzene counterparts. The slightly larger binding energy in TM^+–HQ as compared to TM^+–Bz is attributed to the larger electron density in HQ, which provides more efficient electron transfer to the electron-deficient cationic metal.

For the HQ complexes with the doubly charged metals Pd^{2+}, Pt^{2+}, and Hg^{2+}, efficient L→TM donation (i.e., electron transfer from the ligand to the dicationic metal) is even more important. The ionization energies of the corresponding monocations Pd^+, Pt^+, and Hg^+ are 19.43, 18.56, and 18.76 eV, respectively.[38] Therefore, the charge transfer is accordingly large, and the partial charges on HQ are 1.02, 1.30, and 1.14 in $Pd(HQ)^{2+}$, $Pt(HQ)^{2+}$, and $Hg(HQ)^{2+}$, respectively. We note that in this work, only interaction energies between the two counterparts are considered, since the binding energies with respect to the lowest-energy asymptotes ($TM^+ + L^+$), are not of primary interest. Thus, the resulting dicationic complexes only represent metastable minima on the corresponding potential energy surfaces.

The arguments for the Au^+ complex regarding the change from C_2 symmetry to C_1 also apply to TM^{2+}–HQ, particularly for the heavier 5d elements, where the 6s orbitals are relativistically lowered in energy (see for example reference [41] for a discussion of binding anomalies in Hg^{II} complexes). Pd^{2+} and Pt^{2+} have unoccupied d orbitals which

Table 2. Selected MP2/aVDZ structural parameters of TM^{n+}–L complexes (L = HQ, Bz, Q), given in pm. d_{ring} denotes the length of the TM^{n+}–L distance vector perpendicular to the ligand's plane defined by at least three carbon atoms. For the off-center structures, the distance d_{off} of the TM–L axis (d_{ring}) away from the ring center is also given. d_O is the TM^{n+}–O distance in σ_O complexes. Boldface entries indicate lowest energy structures.

TM^{n+}	L = HQ			L = Bz			L = Q		
	π_{cen} d_{ring}	π_{off} d_{ring}/d_{off}	σ_O d_O	π_{cen} d_{ring}	π_{off} d_{ring}/d_{off}	π_C d_{ring}/d_{off}	π_{cen} d_{ring}	π_{off} d_{ring}/d_{off}	σ_O d_O
Na^+	249		**217**	**241**			270	275/115	**214**
Cu^+	**170**		192	**170**			178	195/108	**189**
Ag^+	**211**			**212**			209	218/111	**213**
Au^+	205	**200/161**	207	206	**202/155**	207/151	209	**196/168**	204
Pd^{2+}	**187**	184/17	241		**163/12**		**167**		198
Pt^{2+}	189	**194/85**	220		**170/72**	163/136	**163**	283/100	191
Hg^{2+}	208	243/174	**265**	211	221/174	**220/185**	213	229/167	**208**

favor the formation of π complexes, and the coordination to oxygen is somewhat less effective. Thus, palladium may slightly more efficiently interact with the ring site, where the π orbitals of the arene ligand may donate into the empty d orbitals of the metal; here, a π_{off} coordination is energetically in close proximity to the centrosymmetric one. Platinum prefers an off-center conformation due to better overlap with the electrophilic, relativistically lowered s orbital. Interestingly, the divalent Hg^{2+} ion on the other hand prefers the σ coordination over the ring site and preferentially binds to the lone pair of the oxygen moiety. Here, the filled 5d shell does not allow the straightforward L→TM π donation, and the high charge density in the dication is best compensated through a directional σ_O bond rather than interacting with a diffuse π-electron cloud.

Pd^{2+} and Pt^{2+} both have triplet ground states with a d^8 configuration giving rise to $^3F_4$ terms. However, for both HQ and Bz, all complexes have singlet electronic ground states. In the benzene complexes of Pd^{2+} and Pt^{2+}, a centrosymmetric C_{6v} structure would result in two singly occupied, degenerate d(e_2) orbitals. Within C_S symmetry, they transform into a doubly occupied d(a′) orbital and an energetically less favorable d(a″) orbital, such that a singlet configuration becomes more favorable over a triplet state. In a π_{cen} structure of the hydroquinone complex, C_2 symmetry applies, and the two highest MOs of the ligand are no longer degenerate. The heavier platinum complex is nevertheless π_{off} bound for more efficient L→TM donation into the low-lying empty 6s orbital of Pt due to the relativistic effect.

Binding of TM^{n+} to Q: For most transition-metal complexes of TM^{n+} to Q, the ring site is less popular than the σ_O coordination. Due to its lower π electron density, quinone is a less effective π donor than HQ. The lone electron pairs of the carbonyl oxygen atoms in Q on the other hand are stronger σ donors than those of the hydroxy groups in HQ. This is also corroborated by the orbital energies of the π-(ring) MOs versus the σ(O) ones: In Q, the σ_O MOs are much closer in energy to the π HOMO than in HQ. Therefore, in the quinone complexes, σ_O coordination becomes more important.

The lighter monocationic quinone complexes with Na^+, Cu^+, and Ag^+ are clearly σ_O-bound (see Table 1). Au^+ still shows a slight preference for π coordination, but the O site is close in energy. Like in the Au^+–arene complexes, the π-coordinated Au^+–Q binds off-center to the ring. Again, symmetry restrictions are responsible for this phenomenon, as in a centrosymmetric complex (which is of C_{2v} symmetry) the π HOMO belongs to the b_1 irreducible representation and does not mix with the 6s(a_1) LUMO of Au^+. In a C_S-symmetric π_{off} structure, both orbitals belong to the same a′ representation such that the electron transfer to the empty 6s orbital of gold is feasible. Due to the high ionization energy of Q (IE = 10.1 eV),[37] the amount of electron transfer from quinone to Au^+ is, however, smaller than that from HQ to the gold cation (q(Q) = 0.15).

Because (unlike the noble metal monocations) the dicationic Pd^{2+} and Pt^{2+} have unoccupied d orbitals, their quinone complexes are of the C_{2v}-symmetric π_{cen} type. Here, the π(b_1) HOMO of Q may donate into an empty d_{xz}(b_1) orbital of the cationic metal. The d^{10} Hg^{2+} on the other hand favors the σ_O site, in analogy to the Hg^{2+}–HQ complex.

Binding of neutral TM to HQ and Q: Upon completion of the redox process, the reduced neutral metal is hosted inside (or plated outside) the oxidized CQ nanotube, where it is in contact with quinone moieties. Generally, the interaction energies of most neutral metals with either Q or HQ are much weaker than in the corresponding cationic complexes, due to the lack of contributions from ion–dipole interactions. Rather, the L→TM π donation and TM→L π* backdonation are the only leading interactions, and π coordination dominates over σ-type bonding. The σ_O coordination is generally not preferred in the neutral complexes. If at all, such structures are the weakest bound, and in the quinone structures, π_{CO} coordination is the preferable site for binding near an oxygen moiety.

The coinage metal atoms have a doublet ground state with a filled d^{10} shell and an unpaired valence s electron. As a consequence, the neutral Cu, Ag, and Au complexes are loosely interacting doublet ground state structures (Table 3), which may be viewed as weakly interacting species with an unpaired electron in a more or less nonbonding HOMO. The mercury complexes are a result of dispersive closed shell–closed shell interactions between a singlet HQ/Q ligand and singlet Hg($5d^{10}6s^2$), which lead to similarly weak interactions. These particularly weak interactions are also reflected in the larger metal–ligand distances in these three complexes (Table 4), as compared to those of the cationic ones, for example, the incremental distance Δd_{ring} = 35, 27, 24, and 60 pm for the copper, silver, gold, and mercury complexes with HQ, respectively.

In marked contrast to copper, silver, gold, and mercury, the neutral palladium complexes are bound more strongly. Formally, a ground state Pd($4d^{10}5s^0$) interacts with a π ligand, such that the ligand's HOMO donates into the

Table 3. Binding energies in kcal mol^{-1} of neutral TM–L complexes (L = HQ, Q) including ZPE contributions and BSSE corrections, calculated at the MP2/aVTZ//MP2/aVDZ level of theory. Values are given only for structures that correspond to the local minima. Boldface entries indicate lowest energy structures.

(TM–L)	L = HQ			L = Q			
	π_{cen}	π_{off}	σ_O	π_{cen}	π_{off}	π_{CO}	σ_O
^{2}(Cu–L)	**1.4**			**12.2**			
^{2}(Ag–L)	2.5	**2.5**		(–0)[a]			**0.0**
^{2}(Au–L)	5.9	**7.2**		**4.1**			0.7
^{1}(Pd–L)	29.2	**34.6**		46.5	**48.5**	35.3	11.0
^{1}(Pt–L)	39.9	**59.8**	20.6	62.5	**76.4**	50.9	35.4
^{1}(Hg–L)	**6.9**		0.6	**4.9**	3.6		0.9
^{3}(Pt–L)	**17.5**			**28.7**			

[a] This value is actually slightly negative (–2.3) due to BSSE. The BSSE-corrected optimal energy conformation would give near zero binding energy.

Table 4. Selected MP2/aVDZ structural parameters of neutral TM–L complexes (L = HQ, Q), given in pm. d_{ring} denotes the length of the TM^{n+}–L distance vector perpendicular to the ligand's plane which is defined by at least four carbon centers. For the off-center structures, the distance d_{off} of the TM-L axis (d_{ring}) away from the ring center is also given. Boldface entries indicate lowest energy structures.

TM	L = HQ			L = Q			
	π_{cen} d_{ring}	π_{off} d_{ring}/d_{off}	σ_O d_O	π_{cen} d_{ring}	π_{off} d_{ring}/d_{off}	π_{CO} d_{ring}/d_{off}	σ_O d_O
Cu	205			**165**			
Ag	254	**246/97**		198			**265**
Au	252	**224/55**		**228**			269
Pd	182	**194/159**		182	**195/149**	189/231	202
Pt	177	**187/172**	202	174	**186/164**	167/262	189
Hg	**303**		368	**333**	**319/126**		324

empty s orbital of Pd, whereas the occupied d orbitals of Pd contribute to the TM→L backbonding. For more efficient p_π–5s donation, the Pd complexes favor an off-center coordination.

The platinum complexes are more strongly bound than the lighter palladium species, because the 6s orbital of Pt is more electrophilic than the 5s orbital of Pd. The singlet states of Pt(HQ) and Pt(Q) are lower in energy than the triplet ones, despite that the ground state configuration of neutral Pt is $^3D(5d^96s^1)$. The promotion to a $^1S(5d^{10}6s^0)$ state is preferred, which costs only 0.24 eV (6.5 kcal mol^{-1}; weighted average over all J, where the energy level for each state is calculated according to Equation (1)); the more compact $d^{10}s^0$ valence configuration allows a closer interaction with the ligand, while at the same time in the π_{off} structure both the efficient electron transfer (to the low-lying 6s orbital of Pt) and the d_π–p_π backbonding are also feasible.

$$E_{avg} = \frac{\sum_{J_{min}}^{J_{max}} (2J+1)E_J}{(2L+1)(2S+1)} \quad (1)$$

In the TM–HQ complexes, Au coordinates to C_1–C_2 such that the HOMO of HQ may donate into the singly occupied 6s orbital of Au, in analogy to the cationic complex. Pt binds to C_2–C_3, but C_1–C_2 coordination is almost isoenergetic—Pt is "ambivalent" in this respect, as it may coordinate either starting from its $5d^96s^1$ ground state configuration or after promotion to the first excited $5d^{10}6s^0$ configuration. The former allows π(HQ)–d_{xz}(Pt) donation, while the latter, allows π(HQ)–6s(Pt) donation. The remaining metals bind to C_2–C_3.

Implications for the self-redox process: In the formation of metal nanowires from the corresponding metal salt, there are several competing factors that are decisive for efficiency or even for mere occurrence of the redox reaction and self-synthesis. Next to the obvious and necessary condition of $E^0(TM^{n+}) < -0.70$ V, which is the pre-requisite for the redox reaction to take place, the most important aspect to be concluded from the energetic properties is the following. All transition-metal cations interact more strongly with HQ than with Q. The relevance of this aspect is immediately clear when considering the stepwise procedure of coordination and electron transfer in the redox reaction. During the coordination process, a transition-metal cation may approach either a HQ or Q moiety. To initiate the redox process, the cation must bind to HQ. Once they are interacting, HQ is oxidized to Q, while the metal cation is reduced to the neutral state. Thus, even if the necessary condition regarding E^0 is met, self-synthesis will only take place efficiently for those metal cations with a binding preference towards HQ over Q.

More importantly, the binding of TM^{n+} with HQ is much greater than that of TM with either HQ or Q, which ensures continuous progress in the self-synthesis. In addition, the interaction energies of the neutral metals either are very weak for both ligands or clearly favor binding to Q. Hence, once the neutral metal is formed, it will not block the interaction sites of the reduced form of the ligand (i.e., HQ), such that the HQ sites are available for the remaining metal cations to be reduced to the corresponding neutrals.

Furthermore, to form 1D nanowire structures, the BE of TM–Q should be smaller than (or at least comparable to) that of a 1D TM nanowire, such that aggregation is favored over formation of isolated TM atoms coordinated to Q. During the growth process, different stages of dimensionality are passed along the way from the initial dimerization step. The resulting cohesive energy per metal atom generally increases from an isolated dimer via a 1D wire and a 2D layer to the three-dimensional (3D) bulk (Figure 4, Table 5).[42–46] Therefore, an initially weak bimetallic interaction may be overcome in a final 1D or 2D metallic array, but encompasses a barrier en route to the metallic product.

The above condition for wire formation, that is, D_0(TM–Q) < BE(1D-TM), is met for Ag (22 ≫ 0 in kcal mol^{-1}), Au (41 ≫ 4) and Pt (77 ≈ 76) [also for Hg (2 ≈ 5)] (Table 5) among the five metals, which satisfy the redox potential condition [$E^0(TM^{n+}) < -0.7$ V]. In the case of Hg, we expect that the nanowire formation would be more likely to be nanorod-like with a few atoms in the cross section, as sug-

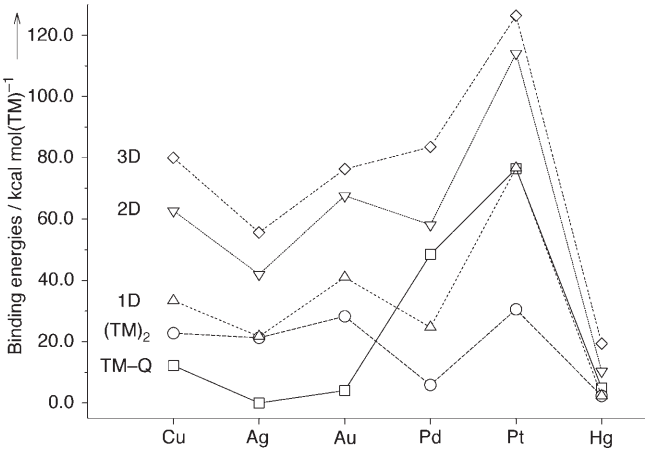

Figure 4. Comparison of binding energies per transition metal for TM–Q, $(TM)_2$, 1D, 2D, and 3D structures of the transition metal.

Table 5. Binding energies of neutral TM with Q and cohesive energies of neutral TM.[a]

TM	TM-Q	$(TM)_2$[b]	(Exptl)[c]	1D[b]	2D[b]	3D[b]	(Exptl)[d]
Cu	[12.2]	22.8	(25.5)	33.4	62.7	80.0	(80.5)
Ag	[0.0]	21.3	(19.0)	21.7	42.0	55.6	(68.0)
Au	[4.1]	28.3	(26.5)	41.0	67.6	76.3	(87.9)
Pd	[48.5]	5.9	(12.5)	24.7	58.1	83.5	(89.7)
Pt	[76.4]	30.6	(36.0)	76.6	114.1	126.4	(134.7)
Hg	[4.9]	2.3	(1.0)	2.3	10.4	19.4	(13.5)

[a] Values in bracktets are from MP2/aVTZ calculations, while the others are from full potential linearized augmented plane wave (FPLAPW) calculations. All energies are in kcal mol$(TM)^{-1}$; thus the binding energy for the dimer per mole of TM is half a dimerization energy. [b] Ref. [42–44]. [c] Ref. [51–54]. [d] Ref. [39].

gested by experiment. In the case of the Ag/Au system, the TM–Q binding energy (0/4 kcal mol^{-1}) is very weak, while both, the dimerization energy (21/28 kcal mol^{-1}) as well as the 1D-TM nanowire formation energy (22/41 kcal mol^{-1}) are large. This indicates that the formation of a metallic nanostructure is favored over formation of isolated metal atoms coordinated to quinone moieties, resulting in effective nanowire formation. On the other hand, for the Pd system, the Pd–Q binding energy (49 kcal mol^{-1}) is much larger than the 1D nanowire formation energy (25 kcal mol^{-1}), which forbids the nanowire formation; thus, the 2D film formation is favored because BE(2D-TM) = 58 kcal mol^{-1} is larger than that of Pd–Q (49 kcal mol^{-1}). As a consequence, metal nanowire growth is expected to occur efficiently for Ag and Au, but not for Pd, while Pt and Hg will exhibit competing behavior between aggregation to nanowires or nanorods and attachment to the ligand. This trend is actually mirrored from the experimental implications.

Conclusion

We have discussed the interactions in transition-metal HQ/Q model systems relevant to the metal nanowire formation in calix[4]hydroquinone nanotubes. In general, the π-bound structures are influenced by symmetry restrictions, which affect charge transfer and orbital interactions; that is, off-center π coordination may throughout be traced back to symmetry constraints in analogy to the TM^+–benzene complexes. In most cationic complexes investigated, ring-bound structures are preferred for HQ due to the synergetic L→TM bonding and TM→L backbonding contributions, while the O-bound species gain their importance in the case of Q; the dicationic mercury complexes favor the σ_O coordination in both cases owing to the high oxophilicity of the mercury dication. Without exception, the HQ complexes are bound more strongly than the corresponding quinone complexes, because the higher electron density in HQ provides more efficient L→TM donation and charge transfer to the electron-deficient metal. For the neutral counterparts, on the other hand, none of the transition metals favors binding near an oxygen site. Rather, all minimum structures are π-bound at the ring-site, and all neutral complexes investigated here are less strongly bound than their cationic counterparts owing to the lack of ion–dipole interactions. While the neutral complexes of silver, gold and mercury are barely bound, palladium and platinum interact with noticeable strength with the respective organic ligands; in the latter two cases, a compact $d^{10}s^0$ valence configuration in the metal, upon complexation, allows a closer interaction with the ligand.

With regard to the real CHQ/CQ system, the model system chosen in this work also explains the efficiency of the overall process in which favorable synergy aspects play a key role. A preferential binding of TM cations to HQ enables efficient initiation of the self-assembly for the redox process to occur spontaneously. At the same time, weak binding of neutral TM species towards either Q or HQ warrants a smooth continuation of the process by ensuring that the coordination sites of still unreacted HQ are preserved for further cationic species to be reduced. Aggregation of neutral TM to form nanowire assemblies is viable if the 1D nanowire formation energy is larger than the TM–L binding energy. Thus, the nanowire formation is most efficient for TM = Ag/Au, but less favorable for TM = Pt/Hg, while Pd cannot form nanowires but it can form 2D layers.

Acknowledgements

This work was supported by KOSEF (CRI) and BK21. Most computations were carried out using the KISTI supercomputers.

[1] P. Tarakeshwar, K. S. Kim, "Nanorecognition", in *Encyclopedia of Nanoscience and Nanotechnology*, *vol. 7* (Ed.: H. S. Nalwa), American Science Publishers, Los Angeles, CA, **2004**, pp. 367–404.
[2] J. C. Ma, D. A. Dougherty, *Chem. Rev.* **1997**, *97*, 1303–1324.
[3] R. A. Kumpf, D. A. Dougherty, *Science* **1993**, *261*, 1708–1710.
[4] K. S. Kim, P. Tarakeshwar, J. Y. Lee, *Chem. Rev.* **2000**, *100*, 4145–4186.
[5] K. S. Kim, J. Y. Lee, S. J. Lee, T.-K. Ha, D. H. Kim, *J. Am. Chem. Soc.* **1994**, *116*, 7399–7400.
[6] J. W. Caldwell, P. A. Kollman, *J. Am. Chem. Soc.* **1995**, *117*, 4177–4178.
[7] E. Cubero, F. J. Luque, M. Orozco, *Proc. Natl. Acad. Sci. USA* **1998**, *95*, 5976–5980.
[8] D. Kim, S. Hu, P. Tarakeshwar, K. S. Kim, *J. Phys. Chem. A* **2003**, *107*, 1228–1238.
[9] D. Feller, *Chem. Phys. Lett.* **2000**, *322*, 543–548.
[10] Y. Mo, G. Subramanian, J. Gao, D. M. Ferguson, *J. Am. Chem. Soc.* **2002**, *124*, 4832–4837.
[11] G. W. Gokel, A. Mukhopadhyay, *Chem. Soc. Rev.* **2001**, *30*, 274–286.
[12] O. M. Cabarcos, C. J. Weinheimer, J. M. Lisy, *J. Chem. Phys.* **1999**, *110*, 8429–8435.
[13] K. S. Kim, P. Tarakeshwar, H. M. Lee, "De novo theoretical design of functional nanomaterials and molecular devices", in *Dekker Encyclopedia of Nanoscience and Nanotechnology, vol. 3* (Eds.: J. A. Schwarz, C. Contescu, K. Putyera), Marcel Dekker, New York, **2004**, pp. 2423–2433.
[14] G. Ashkenasy, D. Cahen, R. Cohen, A. Shanzer, A. Vilan, *Acc. Chem. Res.* **2002**, *35*, 121–128.
[15] A. Niemz, V. M. Rotello, *Acc. Chem. Res.* **1999**, *32*, 44–52.
[16] P. J. Stang, B. Olenyuk, *Acc. Chem. Res.* **1997**, *30*, 502–518.
[17] B. H. Hong, J. Y. Lee, C.-W. Lee, J. C. Kim, S. C. Bae, K. S. Kim, *J. Am. Chem. Soc.* **2001**, *123*, 10 748–10 749.

[18] B. H. Hong, S. C. Bae, C.-W. Lee, S. Jeong, K. S. Kim, *Science* **2001**, *294*, 348–351.
[19] M. H. B. Stowell, T. M. McPhillips, D. C. Rees, S. M. Soltis, E. Abresch, G. Feher, *Science* **1997**, *276*, 812–816.
[20] X. G. Gao, X. L. Wen, L. Esser, B. Quinn, L. Yu, C. A. Yu, D. Xia, *Biochemistry* **2003**, *42*, 9067–9080.
[21] M. L. Paddock, P. H. McPherson, G. Feher, M. Y. Okamura, *Proc. Natl. Acad. Sci. USA* **1990**, *87*, 6803–6807.
[22] C. G. Pierpont, R. M. Buchanan, *Coord. Chem. Rev.* **1981**, *38*, 45–87.
[23] Gaussian 03, Revision B.01, M. J. Frisch, G. W. Trucks, H. B. Schlegel, G. E. Scuseria, M. A. Robb, J. R. Cheeseman, J. A. Montgomery, Jr., T. Vreven, K. N. Kudin, J. C. Burant, J. M. Millam, S. S. Iyengar, J. Tomasi, V. Barone, B. Mennucci, M. Cossi, G. Scalmani, N. Rega, G. A. Petersson, H. Nakatsuji, M. Hada, M. Ehara, K. Toyota, R. Fukuda, J. Hasegawa, M. Ishida, T. Nakajima, Y. Honda, O. Kitao, H. Nakai, M. Klene, X. Li, J. E. Knox, H. P. Hratchian, J. B. Cross, C. Adamo, J. Jaramillo, R. Gomperts, R. E. Stratmann, O. Yazyev, A. J. Austin, R. Cammi, C. Pomelli, J. W. Ochterski, P. Y. Ayala, K. Morokuma, G. A. Voth, P. Salvador, J. J. Dannenberg, V. G. Zakrzewski, S. Dapprich, A. D. Daniels, M. C. Strain, O. Farkas, D. K. Malick, A. D. Rabuck, K. Raghavachari, J. B. Foresman, J. V. Ortiz, Q. Cui, A. G. Baboul, S. Clifford, J. Cioslowski, B. B. Stefanov, G. Liu, A. Liashenko, P. Piskorz, I. Komaromi, R. L. Martin, D. J. Fox, T. Keith, M. A. Al-Laham, C. Y. Peng, A. Nanayakkara, M. Challacombe, P. M. W. Gill, B. Johnson, W. Chen, M. W. Wong, C. Gonzalez, J. A. Pople, Gaussian, Inc., Pittsburgh (PA), **2003**.
[24] T. H. Dunning, Jr., *J. Chem. Phys.* **1989**, *90*, 1007–1023.
[25] M. Dolg, U. Wedig, H. Stoll, H. Preuß, *J. Chem. Phys.* **1987**, *86*, 866–872.
[26] D. Andrae, U. Häußermann, M. Dolg, H. Stoll, H. Preuß, *Theor. Chim. Acta* **1990**, *77*, 123–141.
[27] J. M. L. Martin, A. Sundermann, *J. Chem. Phys.* **2001**, *114*, 3408–3420.
[28] S. F. Boys, F. Bernardi, *Mol. Phys.* **1970**, *19*, 553–566.
[29] *EMSL Basis Set Library*, Environmental and Molecular Sciences Laboratory, Pacific Northwest Laboratory, Richland (WA), Version Feb. 25, **2004**. URL: http://www.emsl.pnl.gov/forms/basisform.html
[30] A. E. Reed, F. Weinhold, *J. Chem. Phys.* **1983**, *78*, 4066–4073.
[31] R. C. Dunbar, *J. Phys. Chem. A* **2002**, *106*, 7328–7337.
[32] M. Diefenbach, H. Schwarz, "Cationic Transition Metal Arene Interactions", in *Encyclopedia of Computational Chemistry*, (Eds.: P. von Ragué Schleyer, P. R. Schreiner, H. F. Schaefer, III., W. L. Jorgensen, W. Thiel, R. C. Glen), Wiley, Chichester, UK, **2004**, DOI: 10.1002/0470845015.cn0091.
[33] G. Frenking, N. Fröhlich, *Chem. Rev.* **2000**, *100*, 717–774.
[34] G. Frenking, K. Wichmann, N. Fröhlich, C. Loschen, M. Lein, J. Frunzke, V. M. Rayón, *Coord. Chem. Rev.* **2003**, *238/239*, 55–82.
[35] T. K. Dargel, R. H. Hertwig, W. Koch, *Mol. Phys.* **1999**, *96*, 583–591.
[36] H. Schwarz, *Angew. Chem.* **2003**, *42*, 4580–4593; *Angew. Chem. Int. Ed.* **2003**, *42*, 4442–4454.
[37] S. G. Lias, J. E. Bartmess, J. F. Liebman, J. L. Holmes, R. D. Levin, W. G. Mallard, "Ion Energetics Data", in *NIST Chemistry WebBook*, *NIST Standard Reference Database*, *vol. 69* (Eds.: P. J. Linstrom, W. G. Mallard), National Institute of Standards and Technology, Gaithersburg (MD), **2001**. URL: http://webbook.nist.gov/chemistry/
[38] W. C. Martin, A. Musgrove, S. Kotochigova, J. E. Sansonetti, "Ground Levels and Ionization Energies for the Neutral Atoms", in *Physical Reference Data*, National Institute of Standards and Technology, Gaithersburg (MD), **2003**. URL: http://physics.nist.gov/PhysRefData/
[39] J. E. Huheey, E. A. Keiter, R. L. Keiter, *Inorganic Chemistry: Principles of Structure and Reactivity*, 4th ed., Benjamin Cummings, San Francisco (CA), **1997**.
[40] P. Schwerdtfeger, M. Dolg, W. H. E. Schwarz, G. A. Bowmaker, P. D. W. Boyd, *J. Chem. Phys.* **1989**, *91*, 1762–1774.
[41] P. Schwerdtfeger, *J. Am. Chem. Soc.* **1990**, *112*, 2818–2820.
[42] T. Nautiyal, S. J. Youn, K. S. Kim, *Phys. Rev. B* **2003**, *68*, 334 071–334 074.
[43] T. Nautiyal, T. H. Rho, K. S. Kim, *Phys. Rev. B* **2004**, *69*, 1934 041–1934 044.
[44] W. Y. Kim, T. Nautiyal, S. J. Youn, K. S. Kim, *Phys. Rev. B* **2005**, *71*, 1131041–1131044.
[45] H. M. Lee, M. Ge, B. R. Sahu, P. Tarakeshwar, K. S. Kim, *J. Phys. Chem. B* **2003**, *107*, 9994–10005.
[46] J. Yoon, K. S. Kim, K. K. Baeck, *J. Chem. Phys.* **2000**, *112*, 9335–9342.
[47] B. C. Guo, J. W. Purnell, A. W. Castleman, Jr., *Chem. Phys. Lett.* **1990**, *168*, 155–160.
[48] F. Meyer, F. A. Khan, P. B. Armentrout, *J. Am. Chem. Soc.* **1995**, *117*, 9740–9748.
[49] Y.-M. Chen, P. B. Armentrout, *Chem. Phys. Lett.* **1993**, *210*, 123–128.
[50] D. Schröder, H. Schwarz, J. Hrušák, P. Pyykkö, *Inorg. Chem.* **1998**, *37*, 624–632.
[51] K. P. Huber, G. Herzberg, "Constants of Diatomic Molecules", in *NIST Chemistry WebBook*, *NIST Standard Reference Database*, *vol. 69* (Eds.: P. J. Linstrom, W. G. Mallard), Natl. Inst. Stand. Tech., Gaithersburg (MD), **2001**. URL: http://webbook.nist.gov
[52] K. A. Gingerich, *Faraday Symp. Chem. Soc.* **1980**, *14*, 109–125.
[53] M. B. Airola, M. D. Morse, *J. Chem. Phys.* **2002**, *116*, 1313–1317.
[54] A. Zehnacker, M. C. Duval, C. Jouvet, C. Lardeux-Dedonder, D. Solgadi, B. Soep, O. Benoist d'Azy, *J. Chem. Phys.* **1987**, *86*, 6565–6566.

Received: December 12, 2005
Published online: May 2, 2006

